Pattern and formation of zonal band structure in forced 2D turbulence on a rotating sphere

AUTHOR(S):

Nozawa, Toru; Yoden, Shigeo

CITATION:

Nozawa, Toru ...[et al]. Pattern and formation of zonal band structure in forced 2D turbulence on a rotating sphere. 数理解析研究所講究録 1996, 972: 183-192

ISSUE DATE:

1996-11

URL:

http://hdl.handle.net/2433/60715

数理解析研究所講究録
972巻 1996年 183-192

Pattern and formation of zonal band structure in forced 2D turbulence on a rotating sphere

京大・理・地球惑星　野沢　徹　(Toru Nozawa)
京大・理・地球惑星　余田 成男　(Shigeo Yoden)

I. INTRODUCTION

For two-dimensional (2D) turbulence on an infinite plane, Kraichnan[1] and Leith[2] theoretically predicted the energy spectrum that has two power laws of k^{-3} in the normal enstrophy-cascading range and of $k^{-5/3}$ in the upward energy-cascading range. Since then many numerical experiments have been done to examine several aspects of the 2D turbulence theory. One of the most remarkable feature of the flow field obtained in the numerical experiments is the emergence of isolated coherent vortices in decaying 2D turbulence[3].

A geophysical application of the 2D turbulence theory was firstly done by Rhines[4] with a numerical model on a β-plane to investigate the effect of rotation of planets on the 2D turbulence. He showed that the upward energy cascade ceases roughly at a characteristic wavenumber $k_\beta = \sqrt{\beta/2U}$, where U is the r.m.s. velocity and β the meridional gradient of the Colioris parameter f. He also found that the flow field becomes anisotropic and a zonal band structure which consists of alternating easterly and westerly jets emerges owing to the β-effect. Shepherd[5] numerically studied the 2D turbulence on a β-plane under the existence of an imposed large-scale zonal jet. He showed that the disturbance energy is transferred into the range of $k \lesssim k_\beta$ owing to the shear-induced spectral transfer, and that the disturbance flow field becomes meridionally anisotropic in this low-wavenumber range.

Recently, Maltrud & Vallis[6] numerically studied the forced 2D turbulence on a β-plane with a high-resolution model (256^2 or 512^2 grids) under recent advanced computing facilities. In their experiments, coherent vortices become weak while anisotropy of the flow field increases as the strength of the β-effect increases. Vallis & Maltrud[7] showed that the obtained zonal band structure is extremely robust and persistent, and that the meridional scale of the obtained zonal jets becomes small as the strength of the β-effect increases. In their experiments, the westerly jets are narrower and sharper than the easterly ones.

Nature of the 2D turbulence in spherical geometry is interesting because of the finiteness of the domain without any artificial lateral boundary, in addition to a possible application to planetary atmospheres. Williams[8] did a series of numerical experiments on the forced 2D turbulence on a rotating sphere, and he reproduced a zonal band structure similar to that of Jovian atmosphere for experimental conditions appropriate to Jupiter. However, the computational domain was restricted to $1/16$ of the entire sphere under the assumptions of longitudinal periodicity and equatorial symmetry, and the forcing function he adopted was not isotropic. Hence, the obtained band structure in the flow field might be influenced by the assumed boundary conditions and the anisotropic vorticity forcing. Recently, Yoden and Yamada[9] did a series of numerical experiments on the decaying 2D turbulence on a rotating sphere to investigate the effects of rotation and sphericity. They found an easterly jet in high latitudes for large rotation rates under the existence of Rossby waves. The initial flow in their experiment has a maximum of energy spectrum

at a relatively low wavenumber $n = 10$ compared with that of the forcing ($n \sim 50$) used by Williams[8], so that the energy transfer in their decaying turbulence may be largely different from that in Williams' forced turbulence.

In this paper, we perform a series of numerical experiments on the forced 2D turbulence in a full spherical domain with a homogeneous and isotropic vorticity forcing to investigate the formation of the zonal band structure from initially zero velocity field. The sensitivity of the formation process to the rotation rate and the forcing wavenumber is studied. The numerical procedure is described in section 2, and results are given in section 3. Discussion is given in section 4, and conclusions are in section 5.

II. MODEL AND NUMERICAL PROCEDURE

Two-dimensional nondivergent flow on a rotating sphere is governed by a vorticity equation :

$$\frac{\partial \zeta}{\partial t} + \frac{1}{a^2} J(\psi, \zeta) + \frac{2\Omega}{a^2} \frac{\partial \psi}{\partial \lambda} = F + \nu \left(\nabla^2 + \frac{2}{a^2} \right) \zeta , \tag{1}$$

where $\psi(\lambda, \mu, t)$ is a streamfunction field, $\zeta(\lambda, \mu, t) = \nabla^2 \psi$: vorticity, λ: longitude, μ: sine latitude, t: time, ∇^2: horizontal Laplacian, $J(\psi, \zeta)$: horizontal Jacobian, a: radius of the sphere, Ω: rotation rate of the sphere, ν: kinematic viscosity coefficient, and $F(\lambda, \mu, t)$: vorticity forcing function. The radius and the rotation rate of the sphere are set to those of Jupiter; $a = 7.00 \times 10^7$m and $\Omega = \Omega_J = 1.76 \times 10^{-4}$rad s^{-1}. Time t is measured by Jovian day; 1 J.day $= 2\pi/\Omega_J = 3.57 \times 10^4$s. The kinematic viscosity coefficient of $\nu = 5.00 \times 10^5$m^{2}s^{-1} is adopted as in Williams[8].

For the forcing function F, a random Markovian formulation is used as in Williams[8]:

$$F(\lambda, \mu, j\Delta t) = RF(\lambda, \mu, (j-1)\Delta t) + (1 - R^2)^{1/2} \hat{F}(\lambda, \mu, j\Delta t) , \tag{2}$$

where R is a dimensionless memory coefficient ($R = 0.98$), and $\hat{F}$ is a randomly generated vorticity source at every time step. The random vorticity source function is defined as follows :

$$\hat{F}(\lambda, \mu, j\Delta t) = \sum_{n=n_f-\Delta n}^{n_f+\Delta n} \sum_{\substack{m=-n \\ m \neq 0}}^{n} \hat{F}_n^m(j) Y_n^m(\lambda, \mu) , \tag{3}$$

where $\hat{F}_n^m(j)$ is an expansion coefficient of $\hat{F}$ with spherical harmonics$Y_n^m(\lambda, \mu)$, which is determined so that it has random amplitude and phase at every time step j in order to construct a homogeneous and isotropic forcing. The forcing is given in a narrow range between $n_f - \Delta n$ and $n_f + \Delta n$ with $\Delta n = 2$, and the r.m.s. amplitude is held constant to F $\equiv \sqrt{\langle \hat{F}^2 \rangle}$ in each run, where $\langle \cdots \rangle$ denotes the spherical average.

A pseudospectral method with a triangular truncation of T199 ($n \leq 199 = N$) is used for the computation of the advection (Jacobian) term; grids for the spectral transformation are 600 in longitudes and 300 in latitudes. Equation (1) is integrated from an initial condition of zero velocity field for a period of $t = 1000$ J.days. The Runge-Kutta-Gill method is used for the time integrations with $\Delta t = 0.05$ J.day. All of the computations are done in double precision.

Table I gives a summary of eighteen experiments which will be reported in this paper. We perform three series of the experiments; three values of the forcing wavenumber $n_f = 20$, 40, and 79 are chosen. For each forcing wavenumber, six values of the rotation rate are chosen: $\Omega/\Omega_J = 0.00$, 0.25, 0.50, 1.00, 2.00, and 4.00. The sphere has Ω/Ω_J rotations par unit J.day.

The r.m.s. amplitude of the forcing F is determined by a method of trial and error to get a similar value of the total energy ($\mathcal{E} \approx 2.45 \times 10^3 \mathrm{m^2 s^{-2}}$) in the cases of no rotation, and the value is not changed for the runs with the same forcing wavenumber.

TABLE I.: Summary of experiments. The column headings are given in the text.

series	run#	n_f	Ω/Ω_J	F ($\mathrm{s^{-2}}$)	$\mathcal{E}$ ($\mathrm{m^2 s^{-2}}$)	n_β
I	1	20	0.00	7.85×10^{-12}	2.46×10^3	—
	2		0.25		2.34×10^3	5.95
	3		0.50		2.23×10^3	8.51
	4		1.00		1.76×10^3	12.77
	5		2.00		8.74×10^2	21.52
	6		4.00		3.97×10^2	37.06
II	7	40	0.00	2.18×10^{-11}	2.45×10^3	—
	8		0.25		2.52×10^3	5.84
	9		0.50		2.45×10^3	8.31
	10		1.00		2.15×10^3	12.14
	11		2.00		1.98×10^3	17.54
	12		4.00		1.03×10^3	29.18
III	13	79	0.00	7.85×10^{-11}	2.43×10^3	—
	14		0.25		2.56×10^3	5.82
	15		0.50		2.51×10^3	8.27
	16		1.00		2.55×10^3	11.65
	17		2.00		2.10×10^3	17.29
	18		4.00		1.64×10^3	25.99

III. RESULTS

The streamfunction field $\psi(\lambda, \mu, t)$ at t = 1000 J.days is shown in Fig.1 for six values of Ω/Ω_J in the series II experiments with n_f = 40. In the case of no rotation (a), the streamfunction field has a very large pattern that is characterized by the lowest wavenumber n = 2 owing to the upward energy cascade. This flow pattern moves irregularly on the sphere without changing the pattern largely. For the experiments with rotation (b-f), on the other hand, zonal band structures become dominant in the streamfunction field. The zonality of the streamfunction field increases as the rotation rate increases. Although details of the flow patterns change with time, the zonal structures do not change particularly for large rotation rates. The amplitude of ψ is large in high latitudes, forming a circumpolar vortex. The edge of the polar vortex shifts to higher latitudes as the rotation rate increases. In the rest of the streamfunction field outside of the polar vortex the amplitude of ψ decreases with an increase in rotation rate, and the zonal band structure becomes unclear in middle and low latitudes for the most rapidly rotating case (f).

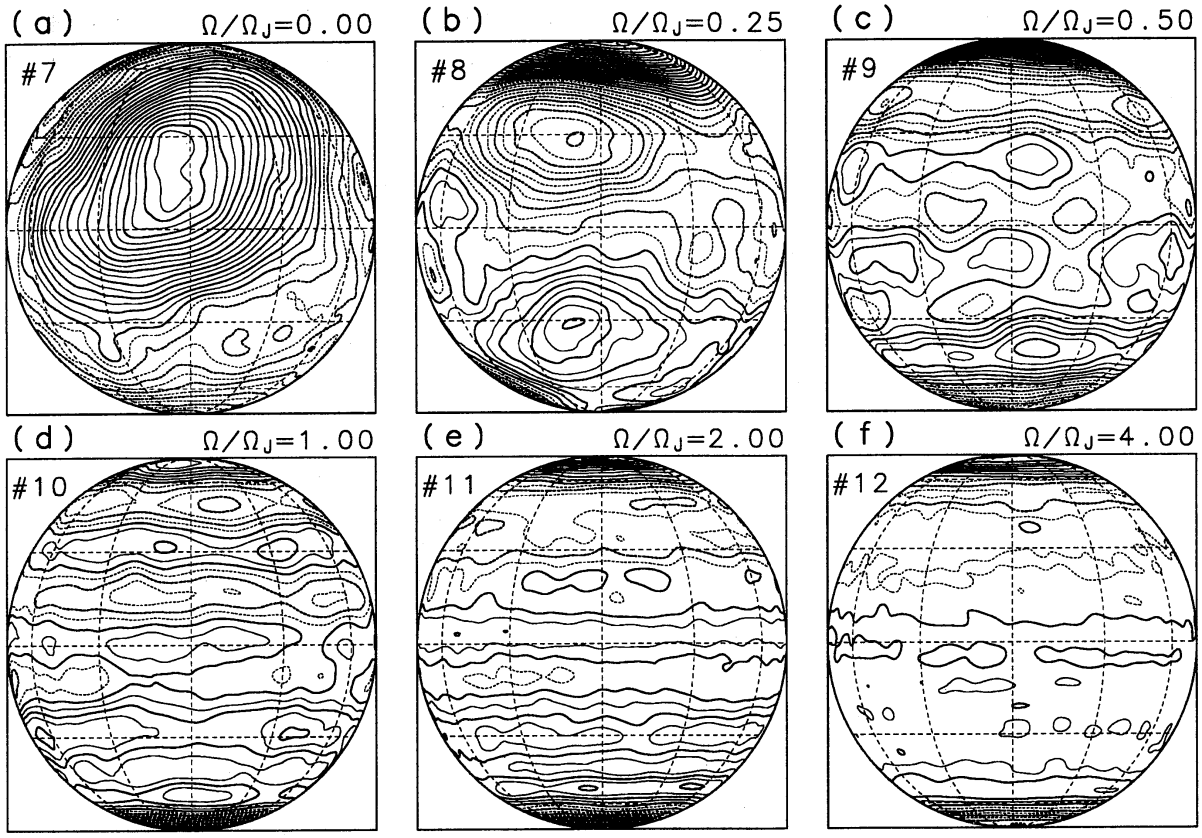

FIG. 1.: Streamfunction field at t = 1000 J.days for the runs of series II. Contour interval is 2.5×10^8 m^{2}s^{-1} and negative areas are denoted by dotted lines. Orthographic projection is used with the center at $\lambda = 0°$ and $\varphi = 0°$. Meridians and parallels are drawn for every 30°.

Figure 2 shows temporal variation of the zonal mean zonal angular momentum $[M] \equiv [u]\, a\sqrt{1-\mu^2}$ for all runs, where $u(\lambda, \mu, t) \equiv -\frac{\sqrt{1-\mu^2}}{a}\frac{\partial \psi}{\partial \mu}$ is a zonal velocity, and $[\cdots]$ denotes the zonal mean. In the cases of no rotation (#1, #7, #13 ; group **A**), the easterly (gray) or westerly (black) flow grows in width as the time goes by, and it dominates over a hemisphere by t = 600 J.days or so. The easterly or westerly bands largely vary their positions with time, corresponding to the irregular movement of the large pattern of ψ as seen in Fig.1 (a). For the cases with rotation, on the other hand, the alternating easterly and westerly zonal bands are already discernible in early stages by t = 100 J.days or so, and do not change their positions largely after the establishment of the band structure. They become clear and robust as the rotation rate increases. These zonal band structures can be classified into two groups: one is the alternating easterly and westerly zonal band structure in all the latitudes (#2-3, #8-11, #14-18 ; group **B**), and the other is the circumpolar easterly jets in high latitudes and weak zonal flow in middle and low latitudes for the experiments with a small forcing wavenumber and a large rotation rate (#4-6, #12 ; group **C**). For the group **B**, the number of the bands increases and their width decreases as the rotation rate increases. For large Ω (#9-11, #17-18), several mergers of westerly bands take place and the width of the bands increases during such events. As the time goes by, there is a tendency that the width of easterly bands becomes broad while that of westerly becomes narrow. For the group **C**, on the other hand, position of the circumpolar easterly jets shifts to higher latitudes with an increase in the rotation rate. The width of the easterly flow becomes broad with time as in the group **B**.

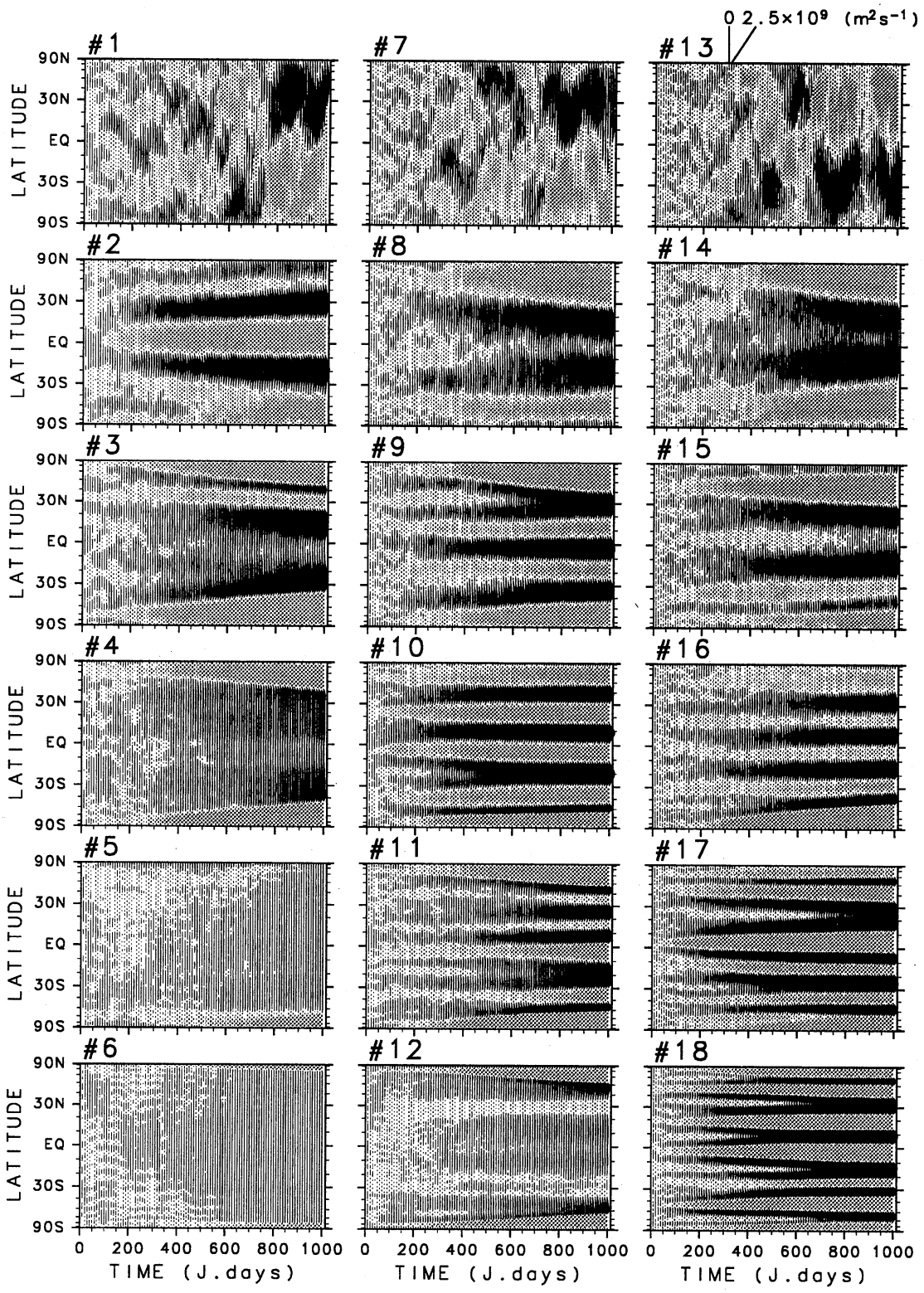

FIG. 2.: Temporal variation of the zonal mean zonal angular momentum. Time interval is 10 J.days, and the unit of an interval is 2.5×10^9 m^2 s^{-1}. Westerly zones are in black while easterly zones in gray. The number in the upper left of each figure represents the run number. The figures are arranged from top to bottom in the order of the rotation rate Ω/Ω_J, and from left to right in the order of the forcing wavenumber n_f.

The dependence of the number of jets on the rotation rate is shown in Fig.3. The number of jets is counted from the time-averaged zonal mean zonal angular momentum for tha last 200 J.days. As seen in Fig.2, the number of jets increases with Ω except for the runs in group **C**, in which the zonal mean flow is weak in middle and low latitudes. For the experiments with the same rotation rate, the number of jets is nearly independent of the forcing wavenumber n_f as far as the alternating easterly and westerly jets emerge in the flow field.

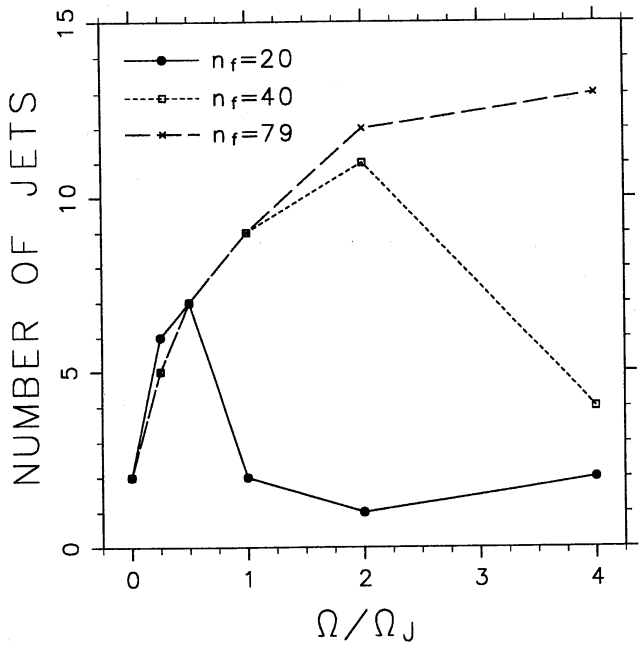

FIG. 3.: Dependence of the number of jets on Ω/Ω_J for the runs of series I (solid circles connected by solid line), for those of series II (squares connected by dotted line), and for those of series III ($\times$s connected by broken line).

Figure 4 shows time-wavenumber sections of energy spectrum density for the disturbance components $E_D(n,t)$ and that for the zonal-mean components $E_Z(n,t)$ for typical three runs of #7, #10, and #12 in the series II experiments. In the case of no rotation (a), the disturbance energy cascades towards the lower wavenumbers as the time goes by, and the spectrum has a maximum at the lowest wavenumber $n = 2$ by $t = 600$ J.days or so. The zonal energy also cascades upward and the spectrum has a peak at $n = 2$ after that time, consistent with the time evolution of $[M]$ (see Fig.2). For the experiment with the rotation Ω_J in group **B** (b), on the other hand, the energy spectrum for the disturbance components has a maximum around $n \sim 10$ after $t \sim 200$ J.days or so, and the distribution of it does not change largely. Here, a characteristic wavenumber n_β is introduced in the analogy of Rhines' k_β[4]:

$$n_\beta \equiv a\sqrt{\langle\beta\rangle/2U}\,, \tag{4}$$

where U is the r.m.s. velocity at $t = 1000$ J.days ($U = \sqrt{2\mathcal{E}}$), and $\langle\beta\rangle$ is the spherical average of β: $\langle\beta\rangle = \frac{1}{2}\int_{-1}^{1}\beta d\mu = \pi\Omega/2a$. At the horizontal scale of a/n_β, the nonlinear Jacobian term is comparable to the "β-term" in Eq.(1). Figure 4 (b) shows that the upward cascade of the disturbance energy ceases around the wavenumber n_β. The distribution of $E_Z(n,t)$ is largely different from that without rotation: the spectral components of the zonal energy, particularly in the low wavenumber range of $2 \leq n \lesssim n_\beta$, begin to increase when the disturbance energy begin to accumulate around the wavenumber n_β. The zonal energy increases with time at several fixed components of the spectrum consistent with the robustness and the persistence of the meridional distribution of $[M]$ as seen in Fig.2. For the run #12 with large Ω of group **C** (c), the time evolution of $E_D(n,t)$ and $E_Z(n,t)$ is rather similar to those in #10 (b). However, the energy upward cascade for the disturbance components is hard to occur because the wavenumber n_β is very close to the forcing wavenumber n_f. Hence, $E_D(n,t)$ has a maximum around the wavenumber n_f for the whole integration period. The disturbance energy penetrates into the low wavenumber range of $15 \lesssim n \lesssim n_\beta$ and the intensity of it varies with time in this range. The number of spectral components at which the zonal energy is dominant is larger than that in #10.

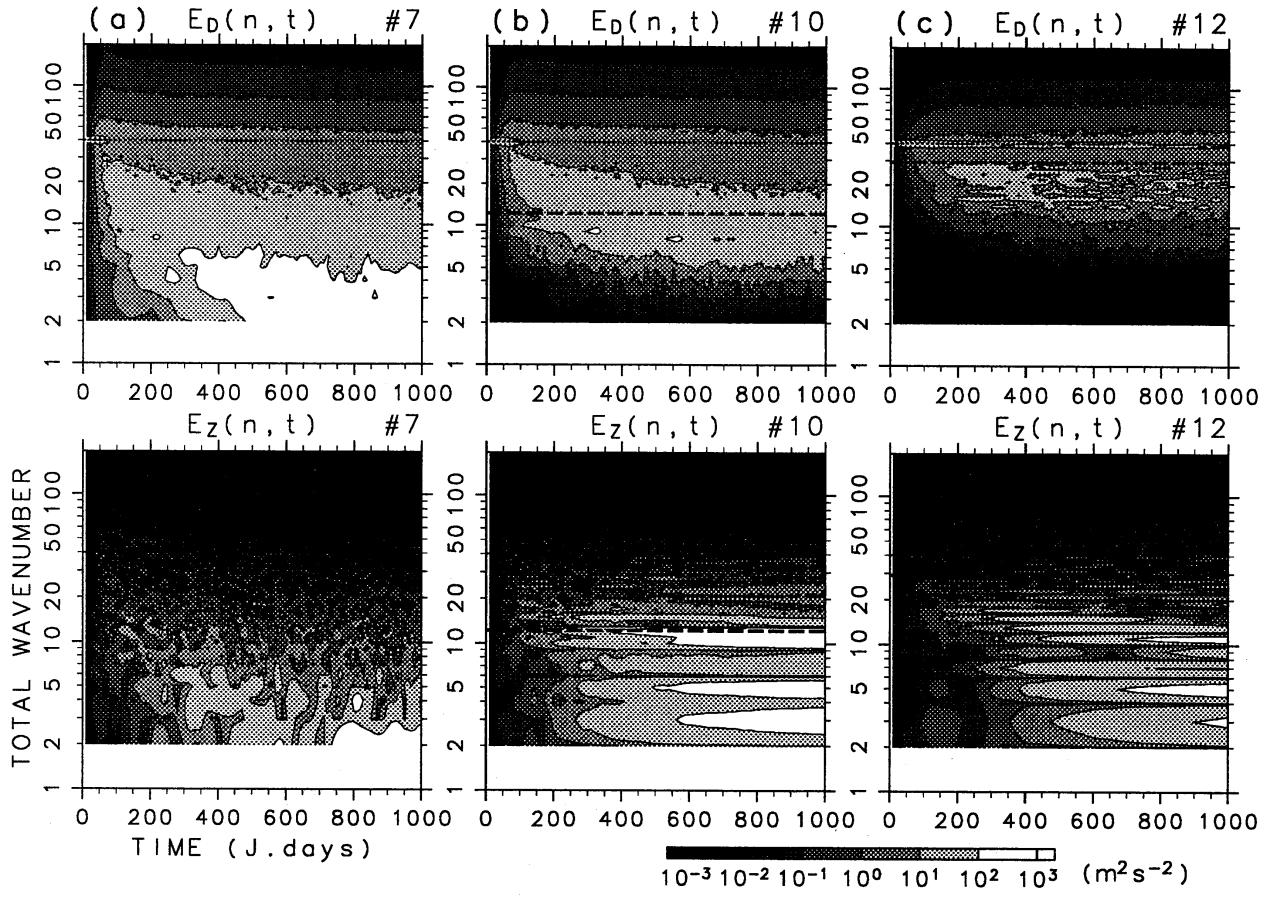

FIG. 4.: Time-wavenumber section of energy spectra for typical three runs of #7 (a), #10 (b), and #12 (c) in series II. Upper figures show the energy spectrum for disturbances and lower ones for the zonal-mean components. Dotted lines indicate the forcing wavenumber (n_f = 40) and broken lines the wavenumber n_β at which scale the "β-term" is comparable to the nonlinear Jacobian term.

Figure 5 shows the relative vorticity field for the disturbance components ζ^* and the zonal mean zonal angular momentum $[M]$ at t = 1000 J.days for the same runs as in Fig.4. In the case of no rotation (a), the disturbance vorticity field is homogeneous and isotropic. The vortex filaments are elongated in various directions insensitive to the distribution of $[M]$. For the experiment with the rotation Ω_J in group **B** (b), on the other hand, the disturbance vortices are elongated by the shear in the mean zonal flow in the whole sphere. This vortex elongation with systematic alignment brings the intensification of the alternating easterly and westerly zonal jets, and corresponds to the energy conversion from the disturbance to the zonal-mean components. For the experiment with large Ω of group **C** (c), the disturbance vortices have nearly circular shape in middle and low latitudes, where the shear of $[M]$ as well as the intensity of it is not very large. Thus the zonal mean zonal flow is not intensified. In high latitudes, on the other hand, the vortices elongated by the strong shear of $[M]$, and the circumpolar jet (,or the polar vortex) is intensified.

IV. DISCUSSION

Yoden & Yamada[9] showed the emergence of strong circumpolar vortices with easterly jets in the numerical experiments on decaying 2D turbulence on a rotating sphere starting from many initial flow fields with the energy spectrum that has a maximum at a low wavenumber n = 10. Similar flow pattern is obtained in this study for the experiment with the forcing wavenumber n_f = 40 and a large rotation rate Ω/Ω_J = 4.00 as shown in Fig.1 (f), and it emerges even for the cases with smaller rotation rate for the smaller forcing wavenumber n_f = 20 (#4-6 in Fig.2). Thus the emergence of the strong circumpolar vortices with easterly jets in their experiments might be due to the smallness of the wavenumber where the energy spectrum has a maximum initially. On the other hand, the most poleward jet (i.e., circumpolar jet) obtained here is easterly for all the runs as seen in Fig.2. Hence the emergence of easterly circumpolar jets in high latitudes seems to be a general feature of both decaying and forced 2D turbulence on a rotating sphere.

The alternating easterly and westerly zonal band structure was found in the numerical experiments on a 2D β-plane turbulence by Vallis & Maltrud[7]. Their experiments showed that the westerly flow is narrower and sharper than the easterly. Similar difference between the westerly and the easterly flow is also seen in this study; the westerly flow becomes narrow and sharp while the easterly becomes wide and gentle as the time goes by (Fig.2). The zonal band structure with narrow westerly and wide easterly is a common feature for the forced 2D turbulence both on a β-plane and on a rotating sphere. Furthermore, in Fig.2, we can see another difference between the westerly and the easterly flow that several mergers of the westerlies take place but merger of the easterlies does not occur in the time evolu-

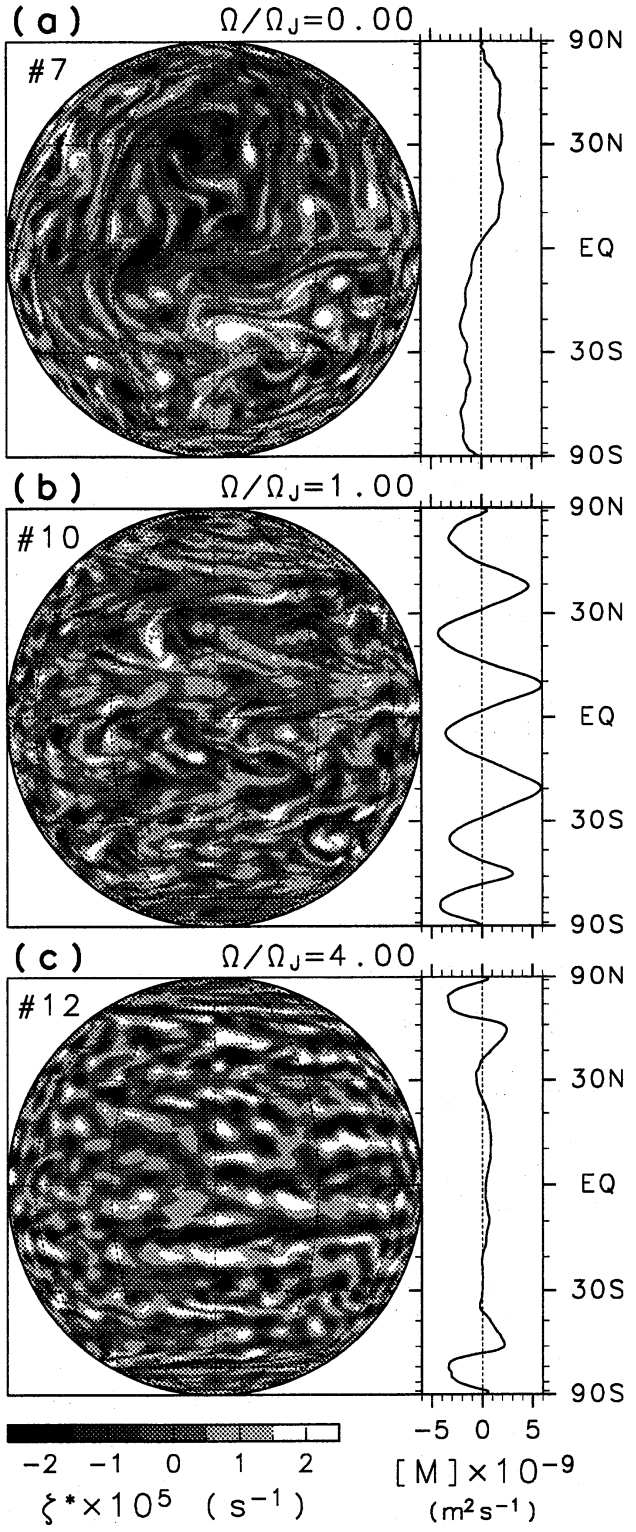

FIG. 5.: Relative vorticity field for the disturbance components (left) and zonal mean zonal angular momentum (right) at t = 1000 J.days for the same three runs as in Fig.4. Map projection is the same as in Fig.1.

tion of the zonal flow field. These difference between the easterly and the westerly flows might be produced by meridionally propagating Rossby wave packets, which may redistribute the zonal mean zonal angular momentum to maintain the band structure resulting in such a remarkable difference.

In the present study, the zonal band structure is formed in early stages and then it becomes robust and persistent for the cases with rotation in group **B** as shown in Fig.2. After the establishment of the band structure ($t \gtrsim 180$ J.days), the disturbance energy is transferred into the zonal mean flow owing to the distortion of the disturbance vortices by the shear in the zonal mean flow as studied by Shepherd[5] in the numerical experiments on 2D turbulence on a β-plane under the existence of an imposed large-scale zonal jet. This straining of the disturbance vortices by the shear seems to be a fundamental dynamics of the formation and maintenance of the band structure for the cases in group **B** as shown in Figs.4 and 5.

For the runs with small rotation rates, the flow field has an alternating easterly and westerly zonal band structure and number of zonal jets as well as width of them is nearly independent of the forcing wavenumber if the value of the rotation rate is identical (e.g. #2, #8, and #14 in Fig.2). On the other hand, the emerged structure is very sensitive to the forcing wavenumber when the rotation rate is large: the alternating zonal bands emerge for the runs with large forcing wavenumber in group **B** while strong circumpolar easterly jets and weak westerly flow in middle and low latitudes emerge for the runs with small forcing wavenumber in group **C**. In group **B**, vortex straining by the shear in the mean zonal flow is dominant in the whole sphere as in the cases with small rotation rate. In group **C**, however, simple Rossby-wave propagation without strong interactions with the mean zonal flow is dominant in middle and low latitudes as seen in Fig.5 (c). This difference in the flow field between group **B** and group **C** suggests the importance of the effect of rotation even in such a small scale of the vorticity forcing.

V. CONCLUSIONS

A series of numerical experiments on the forced 2D turbulence on a rotating sphere were done with a high-resolution barotropic model which has the term of homogeneous and isotropic vorticity forcing. The formation of zonal band structures in the flow field was investigated by sweeping two experimental parameters of the rotation rate and the forcing wavenumber. The process of the formation of a zonal band structure is studied by dividing the vorticity field and the spectral energy equation into the zonal-mean and disturbance components.

In the cases of no rotation (we called group **A**), the streamfunction field shows a very large flow pattern which is characterized by the total wavenumber $n = 2$ because the energy cascades upward to the lowest wavenumber. The easterly or westerly flow dominates over a hemisphere and the zonal bands largely vary their positions with time, consistent with the irregular movement of large coherent vortices in the streamfunction field.

For the experiments with rotation (group **B**), a zonal band structure which consists of the alternating easterly and westerly jets becomes dominant in the streamfunction field. Width of the jets decreases and number of them increases as the rotation rate increases. The band structure is already discernible in early stages of the time integration from the initial condition of no flow field, and it is robust and persistent for the integration period of 1000 Jovian days. The easterly jets become broad and gentle while the westerly ones becomes narrow and sharp.

For the experiments with small forcing wavenumber and large rotation rate (group **C**), the zonal band structure is confined in high latitudes with the emergence of the circumpolar vortex

with strong easterly jets. The position of the circumpolar easterly jets shifts into high latitudes as the rotation rate increases. Outside of the polar vortex, mean zonal flow is weak westerly in middle and low latitudes, and nearly circular vorticity patches are dominant in the vorticity field.

For the runs without rotation, the energy for disturbance components as well as that for the mean zonal flow is transferred to the lowest wavenumber of $n = 2$. For the runs with rotation, on the other hand, the upward cascade of the disturbance energy ceases around a characteristic wavenumber n_β at which the "β-term" due to planetary rotation is comparable to the nonlinear Jacobian term. When the disturbance energy begins to accumulate around n_β, the energy conversion takes place from the disturbance energy to the zonal energy, and the zonal energy increases in the low wavenumber range of $2 \leq n \lesssim n_\beta$. This energy conversion corresponds to the straining of disturbance vortices by the shear in the mean zonal flow, and the elongated vortices with systematic alignment intensify the alternating easterly and the westerly zonal jets.

REFERENCES

[1] R. H. Kraichnan, "Inertial ranges in two-dimensional turbulence," Phys. Fluids **10**, 1417 (1967).

[2] C. E. Leith, "Diffusion approximation for two-dimensional turbulence," Phys. Fluids **11**, 671 (1968).

[3] J. C. McWilliams, "The emergence of isolated coherent vortices in turbulent flow," J. Fluid Mech. **146**, 21 (1984).

[4] P. B. Rhines, "Waves and turbulence on a beta-plane," J. Fluid Mech. **69**, 417 (1975).

[5] T. G. Shepherd, "Rossby waves and two-dimensional turbulence in a large-scale zonal jet," J. Fluid Mech. **183**, 467 (1987).

[6] M. E. Maltrud, and G. K. Vallis, "Energy spectra and coherent structures in forced two-dimensional and beta-plane turbulence," J. Fluid Mech. **228**, 321 (1991).

[7] G. K. Vallis, and M. E. Maltrud, "Generation of mean flows and jets on a beta plane and over topography," J. Phys. Oceanogr. **23**, 1346 (1993).

[8] G. P. Williams, "Planetary circulations: 1. Barotropic representation of Jovian and terrestrial turbulence," J. Atmos. Sci. **35**, 1399 (1978).

[9] S. Yoden, and M. Yamada, "A numerical experiment on two-dimensional decaying turbulence on a rotating sphere," J. Atmos. Sci. **50**, 631 (1993).